EUROPEAN ORGANISATION FOR NUCLEAR RESEARCH

CERN–PPE/96–055
April 23, 1996

The Use of Maximum Entropy in Electromagnetic Calorimeter Event Reconstruction

M.A. Thomson,
CERN, Geneva, Switzerland

Abstract

The method of Maximum Entropy has been applied to the reconstruction of particle positions and energy depositions in the electromagnetic calorimeter of the OPAL detector. The resulting information has been used in the identification of tau lepton decays into pions and ρ mesons. The selection efficiencies and purities compare favourably with those obtained using the standard OPAL reconstruction algorithm.

(To be submitted to Nucl. Inst. and Meth.)

1 Introduction

This paper describes the use of the method of Maximum Entropy in the reconstruction of clusters in the OPAL electromagnetic calorimeter (ECAL). The OPAL barrel ECAL consists of 9440 lead-glass blocks pointing towards[1] the interaction region[1]. The granularity of the calorimeter, $10\,\mathrm{cm} \times 10\,\mathrm{cm}$ at a radius of 2.5 m, is the limiting factor in the identification of semi-leptonic decay modes of the tau lepton. An illustrative example is the separation of $\tau \to \pi\nu_\tau$ and $\tau \to \rho\nu_\tau$ decays. The $\tau \to \pi\nu_\tau$ decays are characterized by a single charged pion which may interact in the ECAL, whereas $\tau \to \rho\nu_\tau$ decays consist of a charged pion accompanied by two photons from the decay of a π^0. Due to the Lorentz boost of the tau lepton, the decay products of the ρ meson are tightly collimated and the electromagnetic deposits from the two photons and the charged pion are typically confined to a few adjacent blocks. Full reconstruction of the pion and photons is only possible if position information below the nominal ECAL granularity is used.

The method of Maximum Entropy has been widely used in the reconstruction of images from astronomical data[2]. Its effect is to improve the granularity of the image and suppress statistical noise. A typical application might involve the reconstruction of data consisting of a number of counts in discrete pixels, with the resulting image being produced with a finer granularity. The situation is analogous to that of event reconstruction in the OPAL electromagnetic calorimeter.

This paper gives a brief introduction to Maximum Entropy and then goes on to discuss how it has been applied to the reconstruction of events in the OPAL ECAL. To demonstrate the possible physics applications the reconstruction is used in the identification of tau lepton decays to pions and ρ mesons. The results show a considerable improvement over the standard OPAL reconstruction where clusters are defined as contiguous sets of ECAL blocks with energies above a certain threshold.

2 The Method of Maximum Entropy

Maximum Entropy is an image enhancement algorithm based on Bayes' theorem. Bayes' theorem is the familiar relationship between joint and conditional probabilities:

$$P(AB) = P(A|B) \cdot P(B) = P(B|A) \cdot P(A), \tag{1}$$

where $P(A)$ is the probability that statement A is true, $P(AB)$ is the probability that both statements A and B are true and $P(B|A)$ is the conditional probability that B is true given that A is true.

The Bayesian approach to statistical analysis is to build in the process of logical induction into the analysis of the data. This is achieved by representing all previous knowledge by a prior probability function and then using Bayes' theorem to describe how the conclusions should be modified in the light of the new data:

$$P(\text{conclusion}|\text{new data}) = \frac{P(\text{conclusion}) \cdot P(\text{new data}|\text{conclusion})}{P(\text{new data})}. \tag{2}$$

[1] The blocks are slightly tilted so as to prevent neutral particles from escaping through the gaps between the blocks.

Since the term $P(\text{new data})$ is a constant (solely a function of the observed data) the above equation reduces to

$$P(\text{conclusion}|\text{new data}) \propto P(\text{conclusion}) \cdot P(\text{new data}|\text{conclusion}). \tag{3}$$

The term $P(\text{conclusion}|\text{new data})$ represents the probability of the conclusion after inclusion of the new data. In the case of image reconstruction the intensities observed in each detector pixel are the new data and the reconstructed image (the conclusion) is chosen to be that which maximizes this term. $P(\text{conclusion})$ is the *prior* probability of the conclusion, *i.e.* the probability assigned to the conclusion before taking into account the new data. It contains all prior knowledge, which might consist of a set of previous measurements or some theoretical expectations. Finally, $P(\text{new data}|\text{conclusion})$ is the probability of obtaining the new data given that the conclusion is true, this is a χ^2-like term comparing the data to the expectation from the conclusion.

In image reconstruction one has some data, which might be number of counts in an array of pixels of a detector, from which it is wished to produce an image, which might be an intensity map with a granularity of significantly less than one detector pixel. In the case of the ECAL reconstruction described below, the data are a set of energy deposits in ECAL blocks and the image is an intensity map which in some way represents the locations and energies of particles incident on the detector.

Let $\mathbf{D}$ be the data and $\mathbf{I}$ be an image (the conclusion), where the data are a set of measurements and the image a set of intensities representing the reconstruction, then from equation 3,

$$P(\mathbf{I}|\mathbf{D}) \quad \propto \quad P(\mathbf{I}) \cdot P(\mathbf{D}|\mathbf{I}). \tag{4}$$

Here, $P(\mathbf{I}|\mathbf{D})$ is the probability of the image, $\mathbf{I}$, after having observed the data, $\mathbf{D}$. It is reasonable to identify the 'best' reconstructed image as the the one which maximizes $P(\mathbf{I}|\mathbf{D})$. The likelihood term, $P(\mathbf{D}|\mathbf{I})$, is the conditional probability of observing the data $\mathbf{D}$ given the image $\mathbf{I}$. This is the familiar χ^2 term. For data consisting of n data points of amplitude A_i with experimental error σ_i this can be written (in the Gaussian limit) as

$$\begin{aligned} P(\mathbf{D}|\mathbf{I}) &= \prod_{i=1}^{n}(2\pi\sigma_i^2)^{-\frac{1}{2}} \exp(-\frac{1}{2}\chi_i^2) \qquad (5) \\ &\propto \exp(-\frac{1}{2}\chi^2), \\ \text{where} \quad \chi_i &= \frac{A_i - A_i^{pred.}}{\sigma_i}. \qquad (6) \end{aligned}$$

The value of χ^2 is calculated by transforming the image, $\mathbf{I}$, into data space using the known experimental resolution (this is just the predicted data distribution, A_i^{pred}, for the image in question). The final factor in equation 4, $P(\mathbf{I})$, is the prior probability of the image. It is this term which selects the best image from the infinite set of images[2] which are consistent with the observed data (*i.e.* those which give an acceptable χ^2).

One choice for the prior probability, $P(\mathbf{I})$, is the 'entropy' term in the method of Maximum Entropy[3],[4],[5]. For the discussion which follows it suffices to state the form

[2]In general, image reconstruction is an under-constrained problem where the number of data points is less than the number of points in the image, and consequently, there will be an infinite set of images which are consistent with the observed data.

of $P(\mathbf{I})$ and to consider its effect on the data analysis. Suppose an image is represented by a set of counts, n_i, recorded in m discrete image pixels then

$$P(\mathbf{I}) = \mathrm{Prob}(n_1, n_2, n_3 \ldots, n_m) \;=\; m^{-N} \frac{N!}{n_1! n_2! n_3! \ldots, n_m!}, \tag{7}$$

where N is the total number of counts. This is simply the combinatorial probability for obtaining a particular configuration if the counts were distributed at random amongst the pixels and is maximal for an equal occupancy in each pixel. For large n_i, equation 7 can be rewritten using Stirling's approximation;

$$P(\mathbf{I}) = \mathrm{Prob}(n_1, n_2, n_3 \ldots, n_m) \;\propto\; \exp(S), \tag{8}$$

$$\text{where} \quad S \;=\; -\sum_i n_i \log n_i. \tag{9}$$

Going from the discrete to continuous case, with counts, n_i, being replaced with intensities, x_i, gives

$$P(\mathbf{I}) \;\propto\; \exp(\kappa S), \tag{10}$$

$$\text{where} \quad S \;=\; -\sum_i x_i \log x_i. \tag{11}$$

and κ is a constant.

The prior probability of the image, $P(\mathbf{I}) \propto \exp(\kappa S)$, is maximum for a uniform distribution. Returning to equation 4, $P(\mathbf{I}|\mathbf{D})$ can now be written as:

$$P(\mathbf{I}|\mathbf{D}) \;\propto\; \exp(\kappa S) \cdot \exp(-\frac{1}{2}\chi^2) \tag{12}$$

$$\;\propto\; \exp(\kappa S - \frac{1}{2}\chi^2). \tag{13}$$

The best image is then chosen to be that which maximizes $P(\mathbf{I}|\mathbf{D})$, *i.e.* that which maximizes $(\kappa S - \frac{1}{2}\chi^2)$. The value of the constant κ determines the relative weights of the χ^2 and entropy terms. Its value is chosen such that the result of the maximization of equation 13 gives a χ^2 of 1 per degree of freedom with respect to the data. The properties of the solutions which maximize equation 13 are summarized below:

- The resulting image is the most uniform solution consistent with the data; the effect of statistical noise present in the data is suppressed in the image.
- Departures from uniformity only arise if there is statistical evidence in the data for such departures. For this to be true the pull of the data (the χ^2 term) must outweigh the pull of the entropy term which favours a uniform solution.
- The image is positive at all points, a desirable feature for cases where negative intensities are meaningless.

3 The Use of Maximum Entropy in the Reconstruction of Clusters in the OPAL Barrel ECAL

In the case of the OPAL Barrel ECAL, the data consist of deposits of energy, $E_{\alpha\beta}$, in $10\,\mathrm{cm} \times 10\,\mathrm{cm}$ lead-glass blocks (subscripts $\alpha\beta$ refer to block coordinates in θ and ϕ). For the purposes of the reconstruction each block was sub-divided into a 10×10 grid. The reconstructed image is a two dimensional set of intensities, x_{ij}, where each intensity is associated with a region of $1\,\mathrm{cm} \times 1\,\mathrm{cm}$.

To apply the technique of maximum entropy it is necessary to calculate both the entropy of the image, which is given by, $S \propto -\sum_{ij} x_{ij} \log x_{ij}$, and the χ^2 term. To determine the χ^2 term one needs to be able to evaluate the expected data distribution, $D_{\alpha\beta}$, for any given image. This depends on the experimental resolution. It is necessary to specify the transformation matrix, $T^{(ij)}_{(\alpha\beta)}$, which maps the image, x_{ij}, to data space, $D_{\alpha\beta}$. The transformation matrix describes how each point in the image would appear in the data. For the reconstruction described below a typical mapping is indicated in figure 1.

The matrix $T^{(ij)}_{(\alpha\beta)}$ is determined from an analytic expression for the expected profile of electromagnetic showers in the lead-glass blocks of the ECAL. Because the lead-glass blocks of the barrel electromagnetic calorimeter approximately point towards the interaction region, only the lateral profile of the showers is important. The lateral energy distribution depends on the Molière radius, R_M, of the material with 90 % of the energy being deposited within a radius of R_M[6, 7]. The lead-glass used in the barrel ECAL has a Molière radius of approximately 3 cm compared to the ECAL block size of $10\,\mathrm{cm} \times 10\,\mathrm{cm}$. As a result, most of the energy of an interacting particle is deposited in a single ECAL block. Information about the position of a particle is predominantly contained in the tails of the distribution, *i.e.* in blocks surrounding the block containing the largest energy deposit. The lateral energy distribution can be parametrized as the sum of two exponential distributions representing core and halo components[8]. Using this parametrization, the expected lateral energy distributions of electromagnetic showers in the OPAL barrel ECAL can be approximated by[9]:

$$f(\rho/\mathrm{cm}) = 0.89(1.81)^2 \exp(-1.81\rho) + 0.11(0.39)^2 \exp(-0.39\rho), \tag{14}$$

where ρ is the radius with respect to the location of the shower origin. This resolution function is appropriate for electromagnetic showers. In the reconstruction no attempt is made to account for the different profile for the energy deposits from charged pions. In the absence of hadronic interactions, charged pions deposit, on average, 700 MeV of energy in the ECAL. Equation 14 is used to determine the energy sharing in a group of 3×3 blocks as a function of the position of the particle in the central block giving the matrix $T^{(ij)}_{(\alpha\beta)}$. The sensitivity of the reconstruction to this parametrization is discussed below. The error, $\sigma_{\alpha\beta}$, on the recorded energy, $E_{\alpha\beta}$, in individual ECAL blocks is assumed to take the form

$$\sigma_{\alpha\beta} = (0.06\sqrt{E_{\alpha\beta}/\mathrm{GeV}} + 0.01)\ \mathrm{GeV}. \tag{15}$$

The first part of the error expression represents the intrinsic energy resolution of the ECAL[1]. The additional term of 0.01 GeV was included to allow an error to be assigned to blocks with no recorded energy.

Given expressions for the transformation matrix $T^{(ij)}_{(\alpha\beta)}$ and the errors on the recorded energies it is possible to construct $\kappa S - \frac{1}{2}\chi^2$ for any image. The maximum entropy solution is obtained by maximizing $(\kappa S - \frac{1}{2}\chi^2)$, which can now be written,

$$\kappa S - \frac{1}{2}\chi^2 \quad = \quad -\kappa \sum_{ij} x_{ij} \log x_{ij} - \frac{1}{2} \sum_{\alpha\beta} \frac{(E_{\alpha\beta} - \sum_{ij} T^{(ij)}_{(\alpha\beta)} x_{ij})^2}{{\sigma_{\alpha\beta}}^2}. \tag{16}$$

The term $T^{(ij)}_{(\alpha\beta)} x_{ij}$ corresponds to the expected data distribution, $D_{\alpha\beta}$, for the image specified by x_{ij}. The maximization of the above non-linear function is performed using the algorithm of Skilling and Bryan[10]. In the maximization procedure the value of κ is chosen such that the image which maximizes equation 16 results in χ^2 per degree of freedom of 1. Due to the iterative nature of the maximization and the large number of calculations involved in determining $T^{(ij)}_{(\alpha\beta)} x_{ij}$ the algorithm is CPU intensive, a single $\tau \to \rho\nu_\tau$ decay takes, on average, 1 second of DEC ALPHA 3000/300LX CPU time.

An example of a maximum entropy reconstruction of a $\tau \to \rho\nu_\tau$ decay is shown in figure 2. The first part of the figure shows the energies deposited in the ECAL by a simulated $\tau \to \rho\nu_\tau$ decay[11]. This information is the $E_{\alpha\beta}$ of equation 16. The second part of the figure shows a contour plot of the maximum entropy reconstruction of these data. This is a contour plot representing the image, x_{ij}. The ECAL energy deposits from the charged pion and from the two photons from the decay of the neutral pion are clearly resolved. It should be noted that to form the final image the only constraints applied are those imposed by the data and the assumptions about the detector resolution contained in the transformation matrix. Apart from the form of the prior probability, no assumptions about the nature of the image are included in the reconstruction.

The image reconstructed by the above procedure consists of an energy-density map in image space (*i.e.* a value for each image cell, where a region of 10×10 image cells corresponds to a single ECAL block). From this image it is necessary to extract clusters which will be identified as energy deposits from particles. This is performed by identifying local maxima in the image as discrete energy deposits from particles. This procedure is reasonable since the entropy term in the maximization forces the image to be as smooth as possible and therefore a local maximum should indicate statistical evidence for a separate energy deposit. The positions of the maxima are used for the positions of the reconstructed clusters. The energies of the clusters are determined by assigning the energy intensity at each point in image space to the closest local maximum. For the case where cells are equidistant from two or more maxima, the intensity of the cell is shared between the clusters associated with the maxima.

4 Study of $\tau \to \pi\nu_\tau$ and $\tau \to \rho\nu_\tau$ Decays

One of the main motivations for the use of Maximum Entropy to reconstruct events in the OPAL barrel ECAL is the efficient separation of different tau decay modes. Of particular practical importance is the separation of $\tau \to \pi\nu_\tau$ and $\tau \to \rho\nu_\tau$ decays[3]. These decays provide an interesting test of the effectiveness of using ECAL clusters reconstructed with Maximum Entropy in a physics analysis. $\tau \to \rho\nu_\tau$ decays consist of three detectable final state particles arising from the decay chain, $\tau^\pm \to \rho^\pm\nu_\tau \to \pi^\pm\pi^0\nu_\tau \to \pi^\pm\gamma\gamma\nu_\tau$. The two photons and the charged pion are typically confined to a few ECAL blocks. The ability to identify these events will depend on the success of the clustering algorithm in separating these closely spaced energy deposits.

In order to reconstruct $\tau \to \rho\nu_\tau$ decays the Maximum Entropy technique is applied to the ECAL information in tau lepton decays from $e^+e^- \to Z^0 \to \tau^+\tau^-$ candidates recorded at OPAL[12]. ECAL clusters reconstructed with Maximum Entropy (local maxima in the image) are assumed to have resulted from energy deposits from charged or neutral

[3] These two channels have the maximum sensitivity to the tau polarization.

particles. Clusters with a high probability of being associated with the tracks present in the event are matched to the tracks. The remaining unassociated clusters are termed neutral clusters and are identified as photons.

To illustrate the discrimination between $\tau \to \pi\nu_\tau$ and $\tau \to \rho\nu_\tau$ decay modes two variables are considered. The first variable is the number of reconstructed neutral clusters. The second variable (which is calculated only for events with one or more neutral cluster) is the invariant mass of the charged pion track and the π^0 candidate, where the π^0 candidate is formed from the two highest energy neutral clusters. Where there is only one neutral cluster, that cluster is taken to be the π^0 candidate. Figure 3 shows the distributions of the number of neutral clusters and invariant mass for Monte Carlo $\tau \to \pi\nu_\tau$ and $\tau \to \rho\nu_\tau$ decays. With only these two variables significant discrimination between the two decay modes can be obtained.

To quantify the improvements over the standard OPAL reconstruction of ECAL events a likelihood ratio technique is used to identify $\tau \to \pi\nu_\tau$ and $\tau \to \rho\nu_\tau$ decays. The likelihoods are based upon kinematic variables reconstructed using Maximum Entropy clusters. For example, if a decay is observed to have no reconstructed neutral clusters, then from figure 3 it can be seen that it is much more likely to be a $\tau \to \pi\nu_\tau$ decay than a $\tau \to \rho\nu_\tau$ decay. The likelihoods from a number of variables are combined and an overall relative likelihood is formed, the value of which is used to identify the decay. Table 1 summarizes the efficiencies and backgrounds for the selections obtained using Maximum Entropy clusters. These results are compared with previously published selections based on: a) the standard OPAL ECAL reconstruction[13], where clusters in the barrel ECAL are defined as contiguous groups of ECAL blocks with energies above 20 MeV, and b) a fine-clustering algorithm optimized for the selection of $\tau \to \rho\nu_\tau$ decays[14]. Significant improvements are obtained when using the Maximum Entropy reconstruction. The predominant background in the selected $\tau \to \pi\nu_\tau$ samples comes from $\tau \to \rho\nu_\tau$ decays. The main background in the $\tau \to \rho\nu_\tau$ samples arises from mis-identified $\tau \to a_1\nu_\tau$ decays (where the a_1 meson decays to a charged pion and two π^0s). These comparisons are not entirely fair since the previous selections were based on hard cuts rather than a likelihood ratio technique. A likelihood ratio selection was performed using the standard ECAL clusters. Efficiencies of 40 % were obtained for both $\tau \to \pi\nu_\tau$ and $\tau \to \rho\nu_\tau$ decays for the same background fractions as obtained when using Maximum Entropy clusters.

	$\tau \to \pi\nu_\tau$		$\tau \to \rho\nu_\tau$	
	Efficiency	Background	Efficiency	Background
Standard Clusters	30 %	7 %	24 %	17 %
Fine Clustering	-	-	58 %	23 %
Standard+Likelihood	40 %	11 %	40 %	23 %
Maximum Entropy	70 %	11 %	74 %	23 %

Table 1: Comparison of different methods to identify $\tau \to \pi\nu_\tau$ and $\tau \to \pi\nu_\tau$ decays. The fine clustering method has not been used for the identification of $\tau \to \pi\nu_\tau$ decays. For the purpose of the comparison, the likelihood selections using the standard ECAL clusters (Standard+Likelihood) are chosen to give the same backgrounds as the Maximum Entropy selection.

The Maximum Entropy reconstruction of tau lepton decays is found to be fairly insensitive to the exact form of the parametrization of the shower profile used to obtain $T^{(ij)}_{(\alpha\beta)}$. To provide a measure of the size of this effect, the reconstruction of Monte Carlo $\tau \to \rho\nu_\tau$ events using the parametrization of equation 14 has been compared to two other cases; the equivalent parametrization with the Molière radius increased by 20 % and the case where contribution from the halo component (the second part of equation 14) was increased by 50 %. For these two cases the mean of the invariant mass distribution for Monte Carlo $\tau \to \rho\nu_\tau$ decays changed by 0.1 % and 0.3 %, respectively. The rms of these distributions changed by 0.6 % and 0.4 %, respectively. In practice, these numbers indicate how inadequacies in the Monte Carlo simulation of ECAL shower profiles might manifest themselves in comparisons of distributions of Monte Carlo and real data.

For the reconstruction to be useful for the analysis of tau lepton decays it is desirable for the Monte Carlo to provide a good simulation of the cluster reconstruction observed in the data. Differences between real and simulated shower propagation could result in undesirable biases. The Maximum Entropy reconstruction method has been applied to both data and Monte Carlo events. Figure 4 shows the distributions of the number of neutral clusters and the invariant mass for selected $\tau \to \pi\nu_\tau$ and $\tau \to \rho\nu_\tau$ candidates for both data and Monte Carlo. The agreement between data and Monte Carlo prediction is excellent, both the mean and rms of the invariant mass distribution for selected $\tau \to \rho\nu_\tau$ decays agree to better than 0.1 %. The performances of the algorithm for data and Monte Carlo events are very similar. Alternatively, this comparison indicates that the shower profile in the ECAL blocks is adequately described by the Monte Carlo.

5 Endcap Reconstruction

One of the strengths of the method of Maximum Entropy for event reconstruction is its adaptability. Maximum Entropy has also been used to reconstruct clusters in the OPAL endcap electromagnetic calorimeter. This detector consists of lead-glass blocks which do not point towards the interaction region[1], thus a single electromagnetic shower traverses a number of blocks. In this case, both transverse and longitudinal shower development are important. By specifying an appropriate resolution matrix, $T'^{(ij)}_{(\alpha\beta)}$, which is now a function of polar angles θ and ϕ, the algorithm can be applied to the endcap calorimeter. Although the reconstruction of endcap clusters has not yet been fully pursued, figure 5 shows an example reconstruction of a Monte Carlo $\tau \to \rho\nu_\tau$ decay in the OPAL endcap ECAL.

6 Conclusions

The method of Maximum Entropy has been used to reconstruct clusters in the OPAL barrel electromagnetic calorimeter. The detector resolution was parametrized by an analytic function representing the transverse profile of electromagnetic showers in the lead-glass blocks of the detector. The effectiveness of the algorithm is shown by significant improvements in the efficiency for identification of $\tau \to \pi\nu_\tau$ and $\tau \to \rho\nu_\tau$ decays over the standard ECAL reconstruction. By providing a different resolution matrix the method has been extended to the OPAL endcap electromagnetic calorimeter.

Acknowledgements

I would like to thank my colleagues on the OPAL collaboration for the successful operation of the OPAL detector, for the development of the Monte Carlo simulation which made this study possible and for allowing OPAL data to be shown is this paper. I also wish to thank David Ward, Gail Hanson and particularly Hal Evans for their comments and suggestions on the text of this paper.

References

[1] The OPAL Collaboration, K. Ahmet et al., Nucl. Inst. and Meth. **A**305 (1991) 275.

[2] see for example;

S.F. Gull, and G.J. Daniell, Nature 272 (1978) 686.

J. Skilling, A.W. Stron, and K. Bennett, Mon. Not. R. astr. Soc. 187 (1979) 145.

R. Willingale, Mon. Not. R. astr. Soc. 194 (1981) 359.

[3] S.F. Gull, and G.J. Daniell, in *'Image Formation from Coherence Functions in Astronomy'* (1979) (ed. C. Van Schooneveld), pp. 219-225, Reidel, Dordrecht.

[4] J. Skilling, in *'Maximum Entropy in Action'* (1990) (eds. B. Buck, and V. Macaulay,), pp. 19-40, Oxford Science Publications.

[5] E.T. Jaynes, in *'Maximum Entropy and Bayesian Methods in Applied Statistics: proc. 4th Maximum Entropy Workshop'*, University of Calgary, 1984, (ed. J.H. Justice,), pp. 26-58. Cambridge University Press.

[6] W.R. Nelson, *et al.*, Phys. Rev. 149 (1966) 201.

[7] G. Bathow, *et al.*, Nuc. Phys. **B**20 (1970) 592.

[8] G.A. Akopdjanov *et al.*, Nucl. Inst. and Meth. **B**140 (1977) 441.

[9] Private communication, M.G. Vincter, A. Astbury, R.K. Keeler and R. Sobie.

[10] J. Skilling and R.K. Bryan, Mon. Not. R. astr. Soc., 211 (1984) 111.

[11] J. Allison, *et al.*, Nucl. Inst. Meth. **A** 317 (1992) 47.

[12] The OPAL Collaboration, G. Alexander, *et al.*, Phys. Lett **B**266 (1991) 201.

[13] M. Sasaki , Proceedings of the 2nd Workshop on Tau Lepton Physics, Ohio State University, Columbus, Ohio 8-11 September 1992.

[14] The OPAL Collaboration, R. Akers *et al.*, Z. Phys. C 65 (1995) 1.

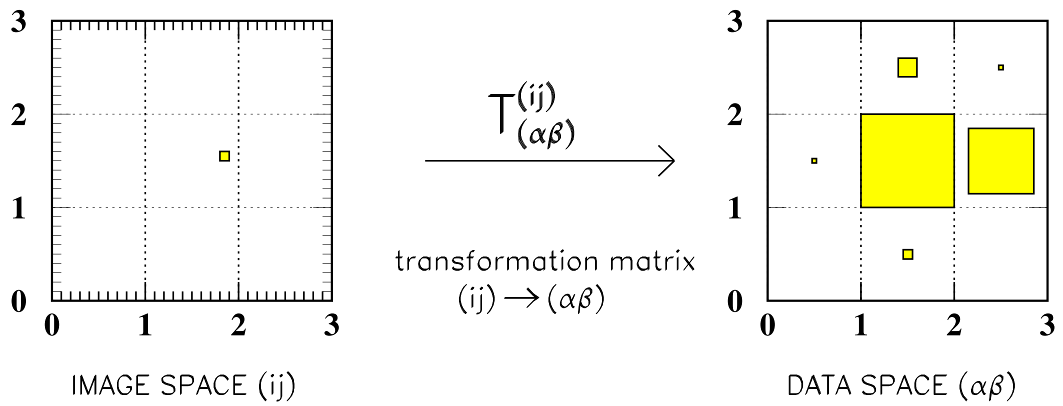

Figure 1: The transformation from the image to data space. The two grids represent a region in the barrel electromagnetic calorimeter consisting of 9 individual lead-glass blocks. In the image each ECAL block has been divided into 10×10 pixels. The shaded pixel in the first plot shows the location in the image under consideration. The transformation matrix $T^{(ij)}_{(\alpha\beta)}$ contains the information about how a particle incident on this image pixel (ij) would deposit its energy in the surrounding ECAL blocks $(\alpha\beta)$. The area of the squares in the right-hand plot indicate the expected fractions of the particle's energy deposited in the blocks.

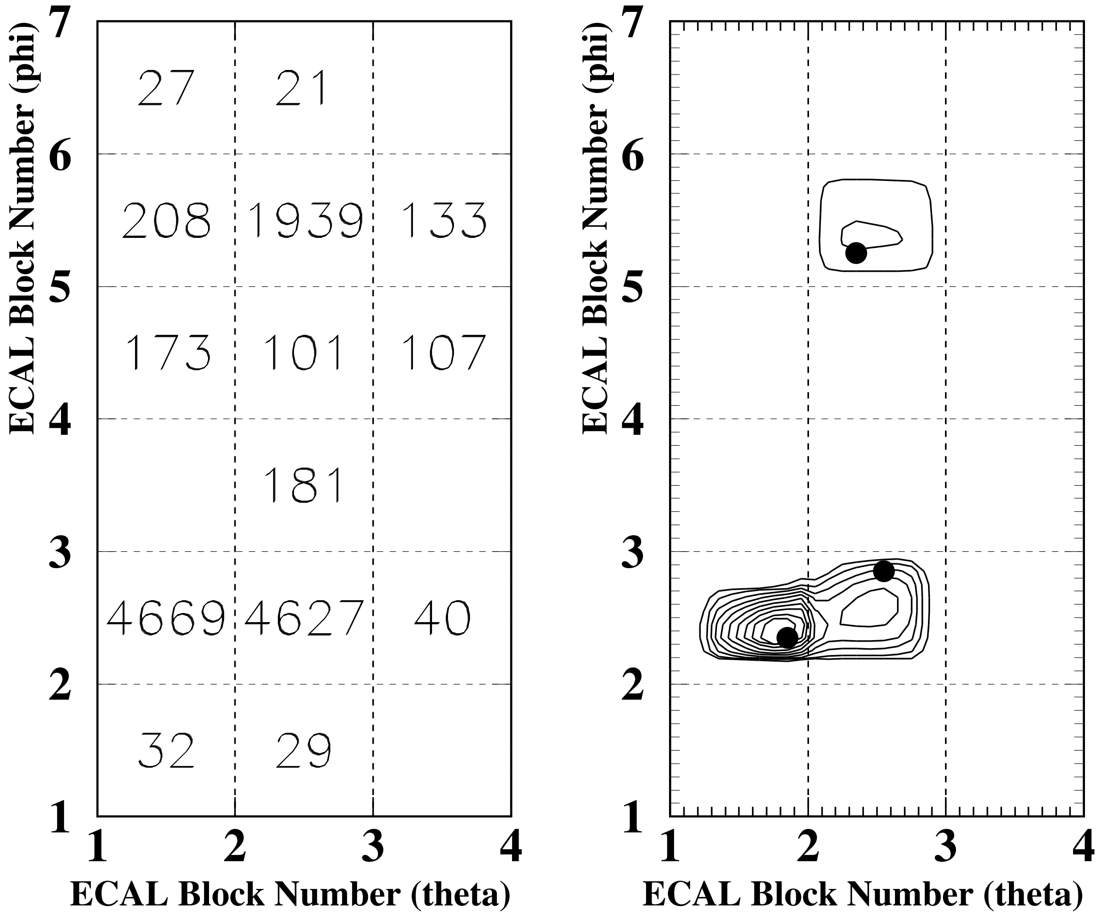

Figure 2: An example reconstruction of a Monte Carlo $\tau \rightarrow \rho\nu_\tau$ decay. The first plot shows the energy (MeV) deposited in the blocks of the electromagnetic calorimeter. Each entry corresponds to the energy observed in a single $10\,\mathrm{cm} \times 10\,\mathrm{cm}$ ECAL block. The blocks outside the region of the plot contain no energy. The second plot shows a contour map of the maximum entropy reconstruction of the event. The contours represent increasing values of the the image intensities, x_{ij}, where each block has been divided into 100 pixels. Also shown in this plot are the true locations of the incident particles. The two lower solid points indicate the positions where the photons from the decay of the π^0 enter the ECAL. The upper solid point shows where the charged pion enters the ECAL. The local maxima of the reconstructed image correspond closely to the true locations of the particles.

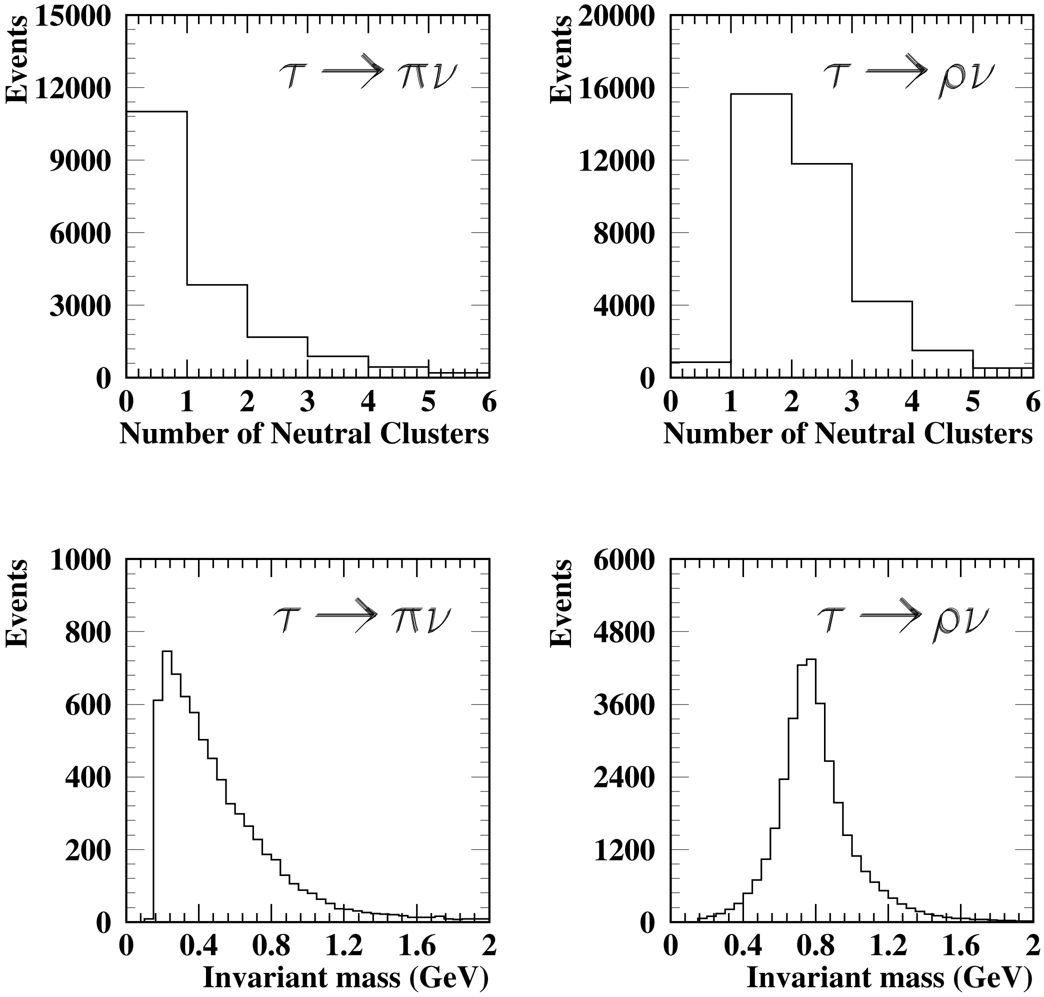

Figure 3: Monte Carlo distributions of the number of neutral clusters and the invariant mass of the track and π^0 candidate where the reconstruction of ECAL clusters has been performed using Maximum Entropy. The invariant mass distributions were made for events with one or more neutral cluster. The reconstruction of most $\tau \rightarrow \rho\nu_\tau$ decays gives one or more unassociated Maximum Entropy cluster. The invariant mass distribution for these events shows a clear peak at the ρ mass.

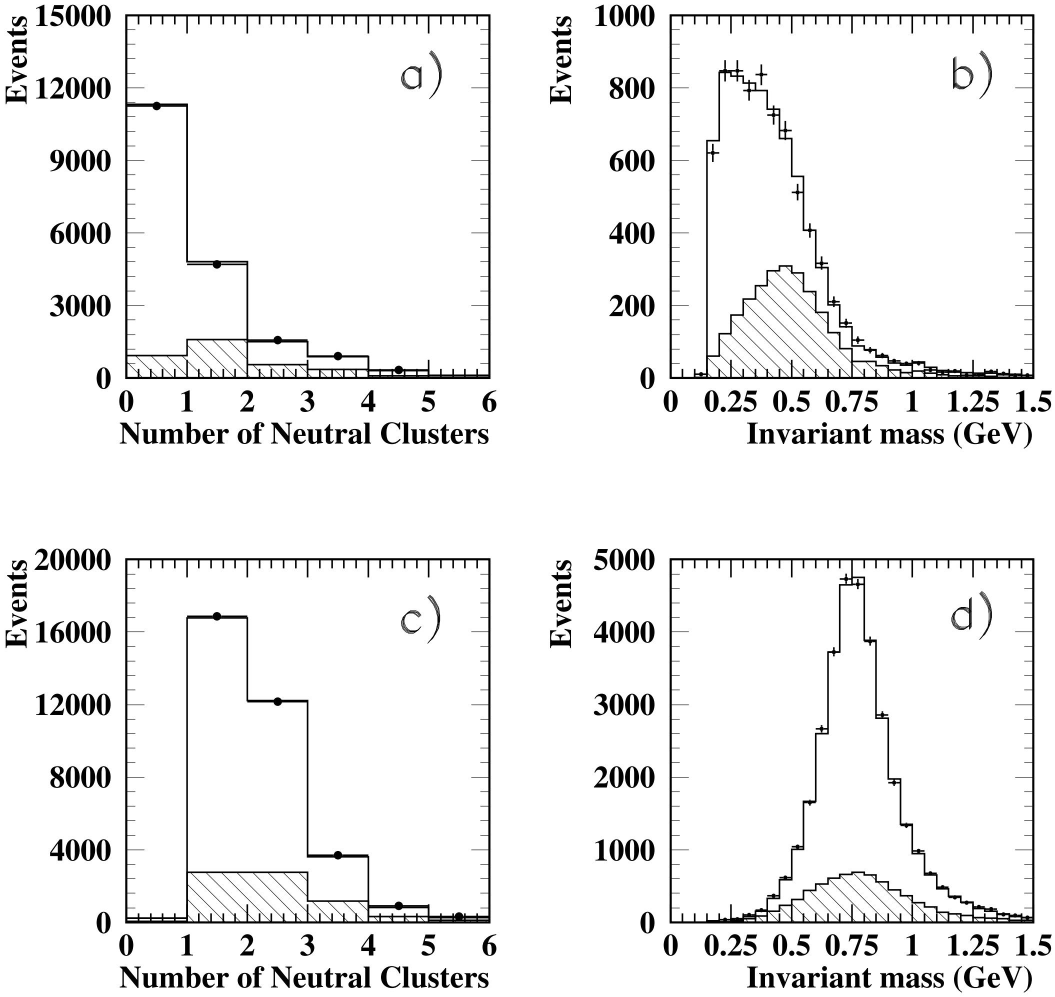

Figure 4: Comparison of data and Monte Carlo distributions for the number of neutral clusters and the invariant mass of the track and π^0 candidate for identified $\tau \rightarrow \pi\nu_\tau$ and $\tau \rightarrow \rho\nu_\tau$ decays. Plots a) and b) show the distributions for selected $\tau \rightarrow \pi\nu_\tau$ events and plots c) and d) show the distributions for selected $\tau \rightarrow \rho\nu_\tau$ events. In each plot, the points or error bars show the data distributions, the open histogram shows the total Monte Carlo expectation, and the shaded histogram shows the contribution from the background from other, mis-identified, τ-decays.

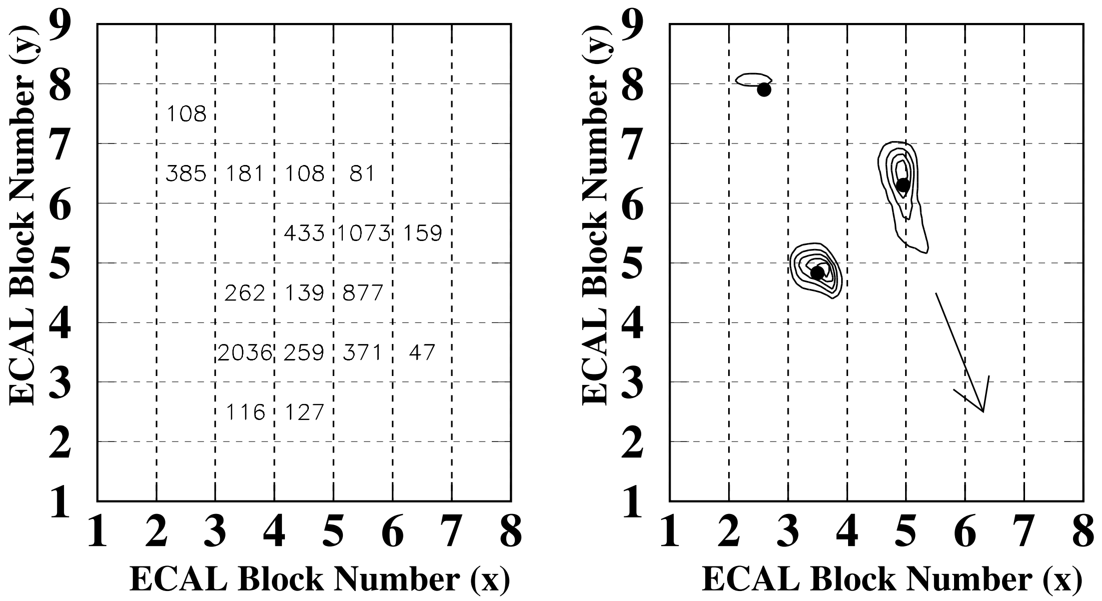

Figure 5: An example reconstruction of a Monte Carlo $\tau \to \rho\nu_\tau$ decay in the endcap ECAL. The first plot shows the energy (MeV) deposited in the blocks of the calorimeter. Each entry corresponds to the energy observed in a single $9.2\,\mathrm{cm} \times 9.2\,\mathrm{cm}$ endcap ECAL block. Because of the non-pointing geometry the direction of the shower development crosses a number of blocks (shown by the arrow on the second plot). The second plot shows a contour map of the maximum entropy reconstruction of the event. The reconstructed maxima are close to the points of incidence of the particles (shown by the solid points). It is worth noting that since the shower development is contained in the matrix, $T'^{(ij)}_{(\alpha\beta)}$, the image maxima correspond to the positions of the incident particles on the front face of the ECAL.